Formation mechanism of a smooth, defect- free surface of fused silica optics using rapid CO_2 laser polishing

[1]**SATCHIDANANDA GHOSH,** *Gandhi Institute of Excellent Technocrats, Bhubaneswar, India*

[2]**PRATYUSH KUMAR,** *Ghanashyam Hemalata Institute of Technology and Management, Puri, Odisha, India*

Abstract

Surface defects introduced by conventional mechanical processing methods can induce irreversible damage and reduce the service life of optics applied in high-power lasers. Comparedto mechanical processing, laser polishing with moving beam spot is a noncontact processing method, which is able to form a defect-free surface. This work aims to explore the mechanism of forming a smooth, defect-free fused silica surface by high-power density laser polishing with coupled multiple beams. The underlying mechanisms of laser polishing was revealed by numerical simulations and the theoretical results were verified by experiments. The simulated polishing depth and machined surface morphology were in close agreement with the experimental results. To obtain the optimized polishing quality, the effects of laser polishing parameters (e.g. overlap rate, pulse width and polishing times) on the polishing quality were experimentally investigated. It was found that the processing efficiency of fused silica materialsby carbon dioxide (CO_2) laser polishing could reach 8.68 $mm^2\ s^{-1}$, and the surface roughness (*Ra*) was better than 25 nm. Besides, the cracks on pristine fused silica surfaces introduced byinitial grinding process were completely removed by laser polishing to achieve a defect-free surface. The maximum laser polishing rate can reach 3.88 μm s^{-1}, much higher than that of the traditional mechanical polishing methods. The rapid CO_2 laser polishing can effectively achieve smooth, defect-free surface, which is of great significance to improve the surface quality of fusedsilica optics applied in high-power laser facilities.

Keywords: laser polishing, mechanical processing, smooth surface, defect-free surface,polishing rate

1. Introduction

The main component of fused silica is silicon dioxide (SiO_2), which has high hardness, low thermal expansion coefficient, and good chemical stability. Fused-silica is mostly used in semiconductors, optical communications equipment, lasers, and other optical instruments due to its excellent thermal, optical, and mechanical properties. In high-power laser facilities, fused silica is used to fabricate ultraviolet optical elements, such as shields (window glass), beam sampling

1

gratings, and focusing lenses [1–3]. However, fused silica optics are susceptible to damage under high-power laser irradiation; and the damaged area increases exponentially with the number of irradiations [4]. The main reason for laser-induced damage of optics is that there are defects located on mechanically processed optical surfaces, such as surface scratches, subsurface microcracks, and impurities [5, 6]. Over the past decades, various ultra-precision technologies have been developed to polish optics, and the defects density has been reduced by several orders of magnitude. However, the efficiency of these ultra-precision processing technologies in removing surface defects is low. The most important issue is that processing-induced defects cannot be eliminated by contact processing. There are some post-processing methods for repairing damaged optics, but the repairing-induced pit modulates the light intensity which damages the downstream optics [7, 8]. When the repairing-induced pit is too large to meet the requirements of beam quality, the optics must be replaced. Therefore, new processing technology is urgently needed to achieve efficient removal of surface defects of optics.

As an advanced manufacturing technique, CO_2 laser polishing is widely used in processing fused silica optics. Fused-silica material has high absorptivity when irradiated by CO_2 laser. The absorption depth varies from 40 to 4 μm as the temperature increases from 300 to 3000 K. As the temperature increases, the material softens, melts, and evaporates. According to this mechanism, CO_2 laser is used firstly to mitigate the surface damage of fused silica optics. With the irradiation of high-power UV laser, the surface of fused silica is damaged, and microcracks are formed in the damage pit. The laser damage resistance of the damaged area is greatly reduced [9, 10]. With the irradiation of CO_2 laser, the material in the damaged area melts or evaporates, the surface quality of the mitigated surface is improved, and the laser damage resistance is greatly improved [11]. CO_2 laser is also applied to fabricate some micro-optical devices. Jung *et al* [12] used CO_2 laser to polish the surface of microfluidic channels and reduced the surface roughness from *Ra* = 172.8 to 67.5 nm. Serhatlioglu *et al* [13] used the same method to reduce surface roughness from *Ra* = 200 to 60 nm. Wlodarczyk *et al* [14] used CO_2 laser to fabricate microstructures on the surface of fused silica in designated areas to form holographic structures, which had good imaging effect. Zhang *et al* [15] used CO_2 laser scanning to produce a uniform periodic structure on the surface of fused silica, and the effect of structural color at a fixed angle was shown. All these prove the potential applications of CO_2 laser polishing in the field of micro-device fabrication. In addition to the local treatment of fused silica, CO_2 laser is also used in processing full-aperture optics. Heidrich *et al* [16] developed a laser-based process chain for full-aperture fused silica optics, including laser rapid prototyping, laser polishing, and form correcting. Using this process chain, they successfully realized the polishing of spherical surfaces of fused silica. The polishing rate of fused silica can reach up to 2.35 $mm^3\ s^{-1}$, and the minimum local polishing depth is as low as 3 nm [17]. After CO_2 laser polishing, the microroughness of a surface decreases from *Ra* = 100 to 0.1 nm [18]. However, for the spatial scale

length of $\lambda > 100$ μm, the surface roughness *Ra* is larger than those processed by traditional mechanical polishing methods. After CO_2 laser treatment, residual waviness with a lateral dimension larger than 100 μm and a vertical dimension smaller than 50 nm remains on the surface, which greatly worsens the surface accuracy. In order to achieve both small roughness and high surface accuracy, laser beam figuring was developed for precision selective material polishing. However, the processed optics hardly used for imaging due to the low surface accuracy and material modification. In particular, residual stress is more likely to induce surface damage under UV laser irradiation [19, 20]. Therefore, let alone the application in high-power laser facilities, CO_2 laser polishing of fused silica still has a long way to go in the field of optical imaging.

In order to investigate the forming mechanism of a smooth, defect-free surface and to predict the surface morph- ology after laser processing, some removal models for rapidly polishing fused silica using CO_2 laser were developed. With laser power density ranging from 99 to 177 W cm^{-2}, Robin
[11] and Doualle [21] used the theory of gaseous thermo-dynamics and dynamics to calculate the polishing depth. The polishing of materials with a removal depth from 0.1 to100 μm was predicted accurately. For a laser power density of 1 MW cm^{-2}, Nowak [22] established a model for calculating
polishing depth by using the Hertz–Knudsen–Schrage formula and energy conservation principle. These studies calculated the
polishing depth after the processing of a single laser beam. However, the mechanism of smooth surface formation under the coupling of multiple laser beams with a high-power laser (1 MW cm^{-2}) has not been reported.

In this paper, a numerical model for predicting the sur-face morphology of fused silica optics fabricated by coupled multiple beams with high-energy density laser is proposed for the first time. The forming mechanism for a smooth, defect- free surface is revealed theoretically. The polishing depth, surface morphology, and surface roughness of laser-polished optics can be calculated by the numerical model. Moreover, the experimental results are in close agreement with the predicted results of the model, which proves that the model can provide theoretical guidance for the optimization of CO_2 laser polishing parameters of fused silica optics.

2. Model and theory

There are many parameters involved in the laser polishing offused silica. In order to optimize processing parameters, it is necessary to study the mechanism of laser polishing theore- tically. The main focus of the reported models is on the polishing depth of the material after a single laser pulse. When the laser beam is moving to process optics, a smooth surface is formed with multiple beams laser polishing. However, the mechanism of surface morphology formation using coupled multiple beams has not been reported.

Laser polishing of fused silica involves multiple physical fields, as shown in figure 1. The fused silica material absorbs energy from the CO_2 laser, and the surface temperature rises rapidly. Heat transfer occurs through heat conduction to the

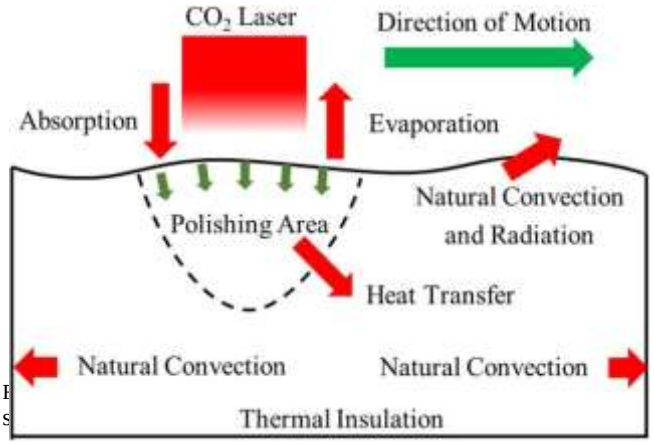

material interior, and heat dissipation occurs through natural convection and radiation at the material interface. Meanwhile, evaporation of materials can also cause energy loss. The process of heat transfer can be expressed as:

$$rC\frac{\partial T}{\partial t} + \nabla \cdot (-k\nabla T) = Q, \tag{1}$$

where ρ is the density of material (2.20 g cm^{-3}), C is the specific heat capacity under constant pressure, T is the temperature, k is the thermal conductivity, and Q is the incident heat source, which can be calculated by:

$$Q(x, y, z, t) = a(1 - R)I_0 \exp\left[-\frac{2(x^2 + y^2)}{r_0^2}\right] \exp(-az), \tag{2}$$

and

$$I_0 = P(t)/(pr_0^2), \tag{3}$$

where $P(t)$ is the time-dependent incident power, r_0 is the radius at 1/e^2 of a Gaussian laser profile, R is the Fresnel reflection coefficient (0.15), and α is the absorption coefficient, which can be expressed by:

$$a = \frac{4pn_k}{l}, \tag{4}$$

where n_k the imaginary part of the refractive index, and λ is the CO_2 laser wavelength.

Laser processing of fused silica is a heat transfer process. That means the material will flow driven by surface tension before evaporation. However, the surface migration due to melt flow can be negligible in a single pulse CO_2 processing with high-power density and short pulse duration. Therefore, the part of morphology changed by melting flow is neglected in the simulation. Laser energy is deposited on the surface of fused silica to form polishing region at high temperature. At this time, the upper surface boundary moves, and the moving mesh is needed for simulation. Geometric deformation of the free surface needs to follow material surface movement. The equation of mesh movement of the free surface can be expressed as follows:

$$(x_t, y_t)^T \cdot n = u \cdot n = v_n, \tag{5}$$

where n is boundary normal vector, $(x_t, y_t)^T$ is the mesh velocity, u is the boundary moving velocity, and v_n is the normal mesh velocity specified in the mesh interface. When the material is evaporated, the gas-solid interface moves toward the solid; and the equation of energy balance of the gas-solid interface can be expressed as follows:

$$r\Delta Hu \cdot n = (F_1 - F_2) \cdot n = \Delta F, \tag{6}$$

where ΔH is the latent heat of evaporation; Φ_1 is the laser energy absorbed by fused silica; Φ_2 is the energy loss of heat conduction in materials, natural convection, and radiation with the environment; and $\Delta\Phi$ is the heat carried away by evaporation of materials.

In the laser-irradiated region, the material temperature reaches the melting temperature T_m, evaporation threshold temperature T_{th}, and evaporation temperature T_v, successively. Elhadj *et al* [23] showed that the evaporation was observed at temperatures in the range of 2600–2800 K, and a few micrometers of material depth could be removed by irradiation over an interval of 4–5 s. Markillie *et al* [24] showed that the analytical prediction was in good agreement with the experimentally observed evaporation threshold when the threshold chosen was 3000 K. The process time scale used by Markillie *et al* was 10–100 μs, which were 6 orders of magnitude shorter than that used by Elhadj *et al*. With the continuous irradiation of the laser, the thermal equilibrium was finally achieved. That is to say, laser energy absorbed by fused silica was equal to the energy loss of internal conduction, boundary convection, radiation, and evaporation. The equilibrium temperature was the material evaporation temperature T_v, which depends on the laser power density [22, 23]. In summary, there are two temperature nodes in laser polishing: evaporation threshold temperature T_{th} and evaporation temperature T_v. The evaporation threshold temperature T_{th} is assumed to be about 3000 K for the pulse width (5–20 μs) of the CO_2 laser used in this work. The evaporation temperature T_v is calculated by [22]:

$$T_v = \frac{2M}{pR_c}\left(\frac{\Delta H}{(1 - R)I_0}\right)^2 (p_s - p_g)^2, \tag{7}$$

where M is the molar mass (60.08 g mol^{-1}) of SiO_2, R_c is the gas constant, p_s is the equilibrium vapor pressure at the temperature of the liquid phase, and p_g is the partial vapor pressure at the temperature of the gas phase [25, 26].

In the process of laser polishing, the region where the temperature exceeds the evaporation threshold temperature is removed. The heat carried by removed material is evaporative heat flux $\Delta\Phi$, which can be calculated by:

$$\Delta F = h_{th}(T_{th} - T) + h_v(T_v - T), \tag{8}$$

where h_{th} and h_v are the heat transmission coefficient of material polishing, which is the function of temperature T:

$$h_{th} = \begin{cases} k_{th}(T_{th}^0 - T) & T \le T_{th} \\ T \ge T_{th}, \end{cases} \tag{9}$$

Table 1. Thermal properties of fused silica used in the calculations.

Density ρ/(kg m^{-3})	Latent heat of evaporation ΔH/(MJ kg^{-1})	Real parts of refractive index (n_i)	Imaginary parts of refractive index (n_k)
2201	12.3	2.363	$1.82 \times 10^{-2} + 10.1 \times 10^{-5}$ (T - 273.15) at 300 K < T < 2100 K

and

$$h_v = \begin{cases} 0 & T < T_v \\ k_v(T_v - T) & T \geq T_v \end{cases}, \quad (10)$$

where k_{th} and k_v are the coefficient; and the k_v is large enough to keep the surface temperature below T_v.

In laser processing, the material removal velocity is transient which is effected by the surface temperature. Therefore, the material removal depth can be calculated by the integration of removal velocity and time:

$$h = \int_0^t v_n \, dt = \int_0^t \frac{h_{th}(T_{th} - T) + h_v(T_v - T)}{\rho D H} dt. \quad (11)$$

The temperature field of material surface can be calculated by heat conduction model, and the surface morphology of material processing will reversely affect the distribution of temperature field. Therefore, a coupled model of surface temperature field and material removal is established. Laser processing, as a kind of thermal action, can remove the surface defects and subsurface defects of materials by evaporating materials. At the same time, there will be no cracks for the noncontact processing method to form a defect-free surface. The thermodynamic parameters of fused silica used in the simulations are shown in table 1.

3. Experiments

The experimental setup for CO_2 laser polishing of fused silica optics is shown in figure 2. A pulsed CO_2 laser source with a maximum output power of $P_{max} \approx 100$ W was used. An external acousto-optic modulator was used for pulse picking as well as to modulate rectangular pulse out of continuous wave laser radiation. The rectangular pulse width ranged from 5 to 100 μs. The focused CO_2 laser moved in a 25 mm ×25 mm area by the control of the galvanometer scanning system. The combined F-Theta lens, with a focal length of 100 mm, focused the diffracted laser beam onto the surface of the fused silica optics. The focused beam had a radius of about 45 μm at 1/e. The maximum velocity of the laser beam was 3 m s^{-1}. Furthermore, the X–Y motion stage moved the fused silica optics in the X and Y directions. It is worth noting that the evaporated SiO_2 powder was absorbed by a suction nozzle to avoid material redepositing on the processed optical surface.

Laser energy was deposited on the surface of the fused silica to form a polishing region at high temperature. With the movement of the laser beam, several polishing pits were coupled to form the surface after laser processing. Figure 3 shows the schematic diagram of the CO_2 laser polishing of fused silica optics. The focused laser beam with average laser

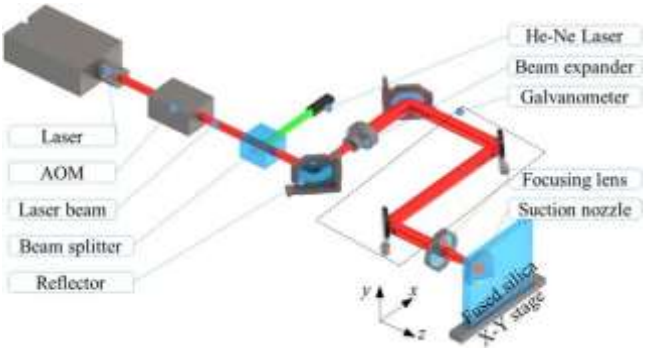

Figure 2. Experimental setup for CO_2 laser polishing of fused silica optics.

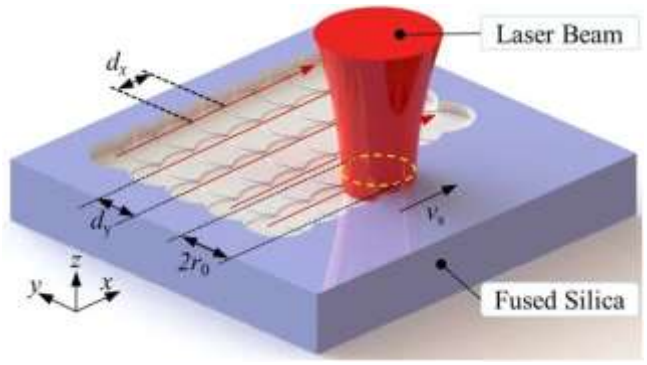

Figure 3. Schematic diagram of CO_2 laser polishing of fused silica optics.

across the surface with the scan velocity v_s in an unidirectional scan strategy, resulting in the pulsed distance d_x, track pitch d_y, and overlap O_x, which can be calculated by:

$$d_x = v_s / f, \quad (12)$$

and

$$O_x = 1 - d_x / (2r_0), \quad (13)$$

To investigate the influence of processing parameters on the polishing quality, the pulse power density E is introduced, which can be calculated by:

$$E = P_a / (\pi r_0^2). \quad (14)$$

power P_a, pulse width t_p, frequency f, and radius r_0 moved

Equation (14) describes the average power of the pulsed-laser-processed area. The parameters investigated in this workare shown in table 2.

The surface morphological details of the processed smooth surface on fused silica optics were examined by a $0.67 \times 0.89\ mm^2$ and $2.2 \times 2.9\ mm^2$ white light interferometer.

Table 2. Parameters used for the experiments of CO_2-laser polishing.

Track Pitch d_y/(mm)	Scan speed v_s/(m s^{-1})	Frequency f/(kHz)	Laser power P_a/(W)	Pulse width t_p/(μs)
0.03	0.05–0.9	1–10	50	5–10

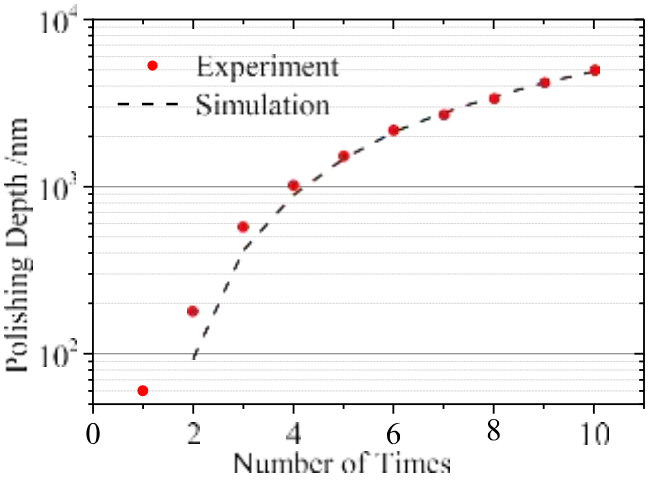

Figure 4. Polishing depth as a function of polishing times, for a beam radius of 45 μm. The black dashed lines are the simulation results based on the model described in section 2.

The surface defects were observed by scanning electron microscopy (SEM) and high-magnification optical microscope.

4. Results and discussion

Depth of laser polishing

In order to verify the accuracy of the laser polishing model, the simulation results were compared with the experimental results. Firstly, the model was refined. The experimental parameters of the laser with power of 50 W, pulse width of 10 μs, and number of 10 were used to polish fused silica. It is worth noting that the effective pulse width was 9.5 μs because of the rising edge and the falling edge of laser pulse. Moreover, part of the laser energy was absorbed by evaporated SiO_2 in the polished area, which led to an energy loss with a loss coefficient of 0.75.

Figure 4 shows a comparison of the polishing depth between the simulation and experiment, and the abscissa represents the number of laser polishing. After the first pulse laser heated, the maximum surface temperature of the fused silica was about 2600 K, which was below the evaporation threshold temperature. However, surface modification occurred, i.e. the fictive temperature and material density increased [19, 25]. As a result, a pit was formed by material densification in the experiment, while the simulation results show that the material did not evaporate. When the polishing depth was greater than 500 nm, the simulated and experimental results were in good agreement.

Mechanism of surface formation

Laser polishing of fused silica is a thermal process, which is equivalent to the thermal grinding head in mechanical processing. Within a processing cycle T_p:

(a) Within the pulse width t_p, the material absorbs laser energy and rapidly reaches the polishing state to achieve evaporation removal of the material.
(b) When the laser is turned off and the material is cooled for a period of time (T_p-t_p), the surface temperature decreases.
(c) The laser beam moves a pulsed distance d_x to the next processing position.
(d) The above steps are repeated.

The processing area is equivalent to the superposition of thousands of laser beam removals. Therefore, it is necessary to investigate the material removal depth and the surface temperature distribution after each pulse laser.

The temperature distribution in the fused silica optics after laser polishing is shown in figure 5. The results were simulated by commercial software with a power of 50 W, pulse width of 10 μs, frequency of 10 kHz, and a pulsed distance of 27.7 μm (overlap O_x = 69.2%). The surface temperature gradient was very high when the pulsed-laser-irradiated on the surface of fused silica. After cooling, the surface temperature of the material decreased rapidly; and the maximum temperature on the surface was below 2600 K after nine pulses.

The maximum surface temperature in laser polishing of fused silica optics is shown in figure 6. The evaporation temperature T_v was about 3400 K while the pulse power density E = 0.786 MW cm^{-2}. After irradiation by the laser beam, the surface temperature decreased to less than 3000 K within a few tens of microseconds. Thereafter, the material was no longer removed. At the same time, when the number of laser pulses reached four, the maximum surface temperature kept stable at 2600 K at the end of cooling. This shows that the heat exchange was stable after four laser pulses, and CO_2 laser polishing was a steady removal process.

The evolution of the surface morphology of fused silica optics with laser beam motion is shown in figure 7. The solid line is the surface morphology formed after each laser pulse irradiation, and the dashed line is the irradiation position of the laser beam. The results show that the surface morphology expanded uniformly to the right, the maximum polishing depth was 618 nm, and the residual height of polishing morphology was 26 nm after irradiation of four laser pulses. Therefore, polishing surface morphology can be predicted at any time thereafter. In addition, the peak of polishing morphology was in the position of two consecutive laser pulses but not in the middle position. The position was related to the laser processing parameters, which is not discussed in detail here.

Above all, the temperature distribution and the morphology of the processed surface with the moving laser polishing was obtained. Laser polishing of fused silica is a thermal,

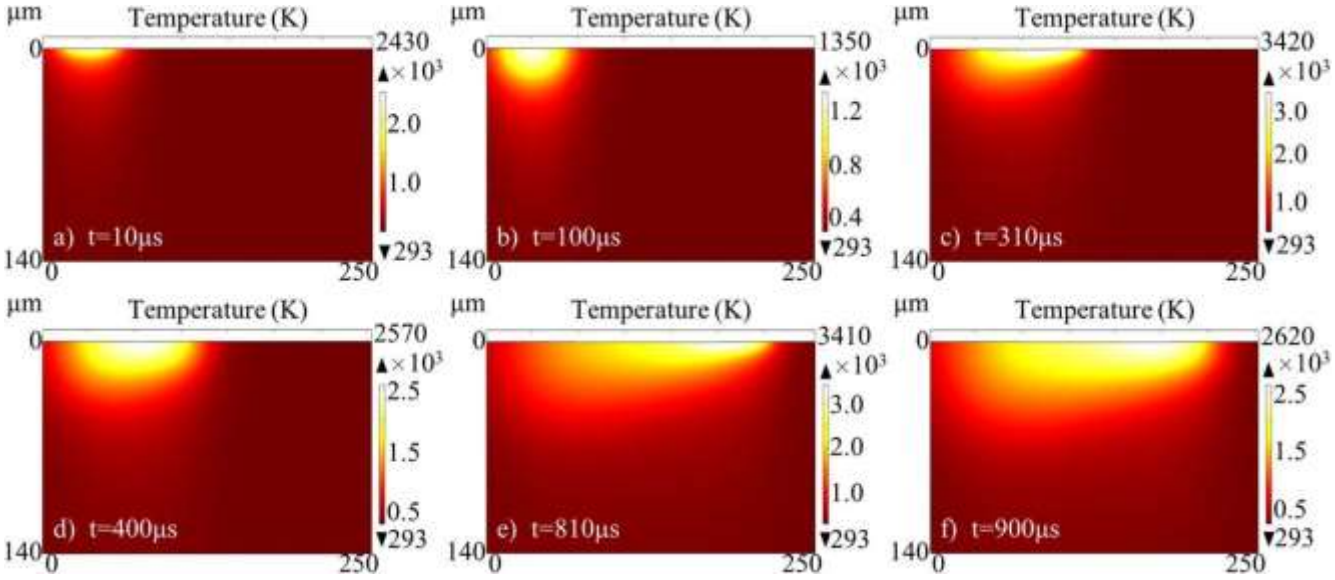

Figure 5. The temperature distribution in the fused silica optics after: (a) first pulse laser polishing, (b) first cooling, (c) fourth pulse laser polishing, (d) fourth cooling, (e) ninth pulse laser polishing, and (f) ninth cooling.

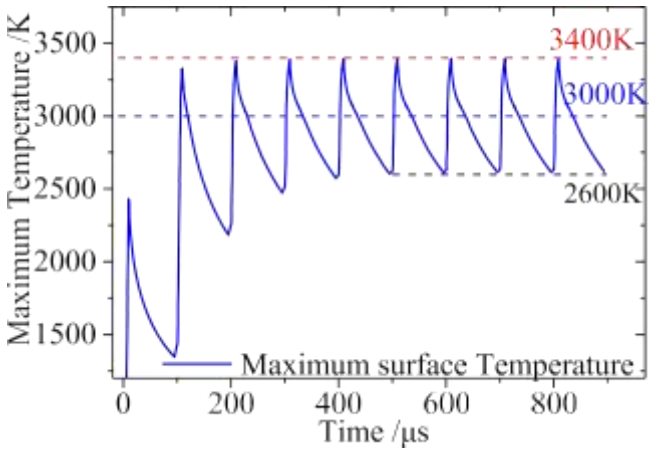

Figure 6. The curve of the maximum surface temperature in the laser processing optics.

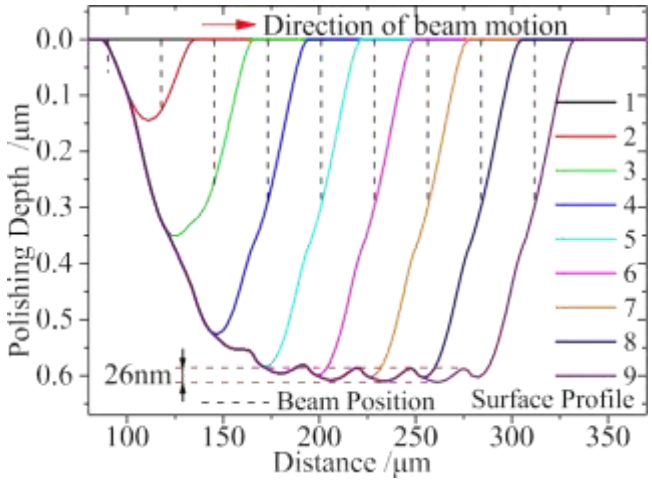

Figure 7. Evolution of surface morphology of fused silica optics with laser beam moving.

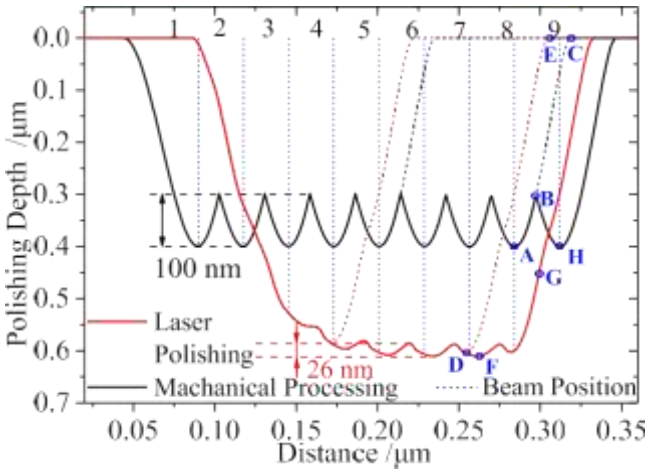

Figure 8. Comparison of the formation mechanisms of surface morphology between mechanical processing and laser polishing.

noncontact process, while mechanical processing is a contactprocess. A comparison of the formation mechanisms of surface morphology between mechanical processing and laser polish-ing is shown in figure 8. It is assumed that the polishing removal volume of a single laser pulse is the same as that of a single tool. The black and red curves in the figure are the processed surface morphology after mechanical processing and laser polishing, respectively. At the beginning of laser irra- diation, the polishing depth was shallow, which formed inho- mogeneous polishing morphology on the surface. When the polishing morphology was uniform, the formation mechanisms of surface morphology between laser processing and mechan- ical processing was different. Mechanical processing, a contact process, removed materials from the contact area. As shown in
figure 8, surface B–C expanded to surface B–H, while the untouched surface A–B did not change after mechanical processing. The laser, a high-energy electromagnetic wave,

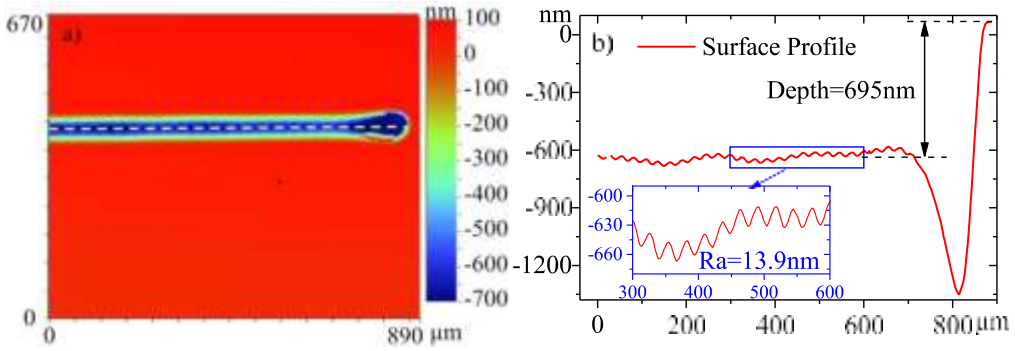

Figure 9. White light interferometry images of the laser-polished field, (a) and the surface profile along the dashed line (b) using the parameters of laser processing with a power of 50 W, pulse width of 10 μs, frequency of 10 kHz, and a pulsed distance of 27.7 μm.

deposited on the material surface in its propagation direction. Therefore, surface D–E in figure 8 extended to surface D–F–G after laser polishing. It is worth noting that the wave front of the laser polishing was delayed more than that of mechanical processing. This is because the wave front material absorbed heat.

After understanding the forming mechanism of the laser polishing surface, the roughness *Ra* of the residual surface was calculated theoretically by:

$$Ra = \frac{\sum_{i=1}^{N} |x_i - \bar{x}|}{N} \quad (15)$$

The theoretical calculation showed that the roughness *Ra* of the laser polishing surface was 6.94 nm. Therefore, it was necessary to optimize the relevant parameters so that the surface had the smallest roughness without reducing the efficiency of laser polishing. This is the way to produce a smooth surface. Moreover, laser polishing had no cutting force and could produce surfaces without surface scratches and other defects.

Evaluation of surface quality

The formation mechanism of the smooth surface of optics has been revealed. The polishing depth, surface morphology, and surface roughness of optics after laser polishing were theoretically obtained. In order to verify the accuracy of the model, we carried out relevant experiments. Figure 9 shows the experimental results after laser polishing of fused silica optics. Some differences between the experiment and simulation were observed. The densification of materials was not considered in the simulation, which resulted in the polishing depth in the experiment (695 nm) being deeper than that in the simulation (618 nm). The error was about 11%. However, when the overlap of the laser beam was increased to 76.9%, the polishing depths obtained by the experiment and simulation were 1387 and 1343 nm, respectively. The error was reduced to 3.2%. The microstructure remained on the surface after laser processing. The period of the microripple was 27.3 μm, which was approximately equal to the pulsed distance of 27.7 μm. The microripple with a height of 23 nm was slightly smaller than the simulated result of 26 nm, which was induced by the fluid flow. Noticeably, the fluid flow that occurred for the surface temperature was greater than 2300 K, which is the melting point of fused silica. Ultimately, the polished surface quality deteriorated, and the surface roughness *Ra* detected was 13.9 nm, higher than that calculated in section 4.2. However, the roughness 13.9 nm was smooth enough to improve the surface quality after grinding. In summary, the experimental results were in good agreement with the simulation results.

In order to show the smooth surface of laser polishing, surface polishing on the fused silica surface was carried out. The laser parameters with a power of 50 W, frequency of 10 kHz, pulsed distance of 27.7 μm, and track pitch of 30 μm

were used to polish fused silica optics. With this parameter, the surface processing efficiency of laser polishing of fused silica reached 8.68 $mm^2\ s^{-1}$. Figure 10 shows the profile after laser polishing of fused silica with different pulse widths. From 5 to 10 μs, the polishing depth were 53.5, 130, 1202, and 2414 nm and surface roughness *Ra* were 2.68, 3.22, 14.46, and 24.8 nm, respectively. In addition, with the increase of pulse width, the laser polishing depth increased exponentially, i.e. the material removal efficiency of laser processing increased rapidly. The surface roughness *Ra* of laser polishing was better than 25 nm, which realized the processing of a smooth surface of fused silica optics.

Removal of surface and subsurface defect

The formation mechanism of a smooth surface was revealed theoretically and verified by experiments. It was necessary to further verify the elimination of residual defects on the sur- face of fused silica optics after laser polishing. A rapid CO_2 laser polishing technique provided an alternative technology for precision polishing of fused silica optics, so it was used to process ground optics. The grinding optics, with a roughness of 250 nm and a large number of cracks, was polished by CO_2 laser to investigate the removal of surface and subsurface defect. Figure 11 shows the surface measurements by SEM before and after laser polishing with a pulse width from 5 to 10 μs. The parameters of laser polishing were a power of 50 W, frequency of 10 kHz, pulsed distance of 20.7 μm, and track pitch of 17.3 μm. The surface became smooth after laser polishing with a pulse width of 5 and 6 μs; but there were still some cracks on the surface, as shown in the lower half of

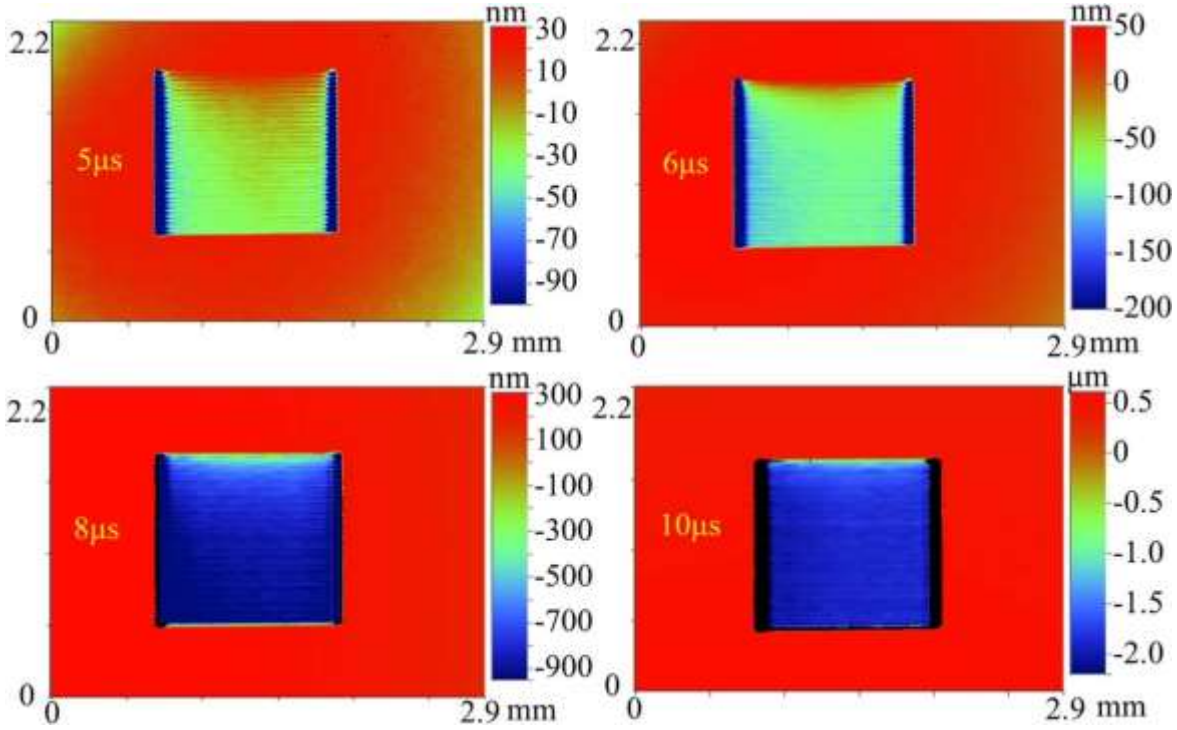

Figure 10. White light interferometry images of laser-polished field using the parameters of laser polishing with power of 50 W, frequency of10 kHz, pulsed distance of 27.7 μm, track pitch of 30 μm, and a pulse width from 5 to 10 μs.

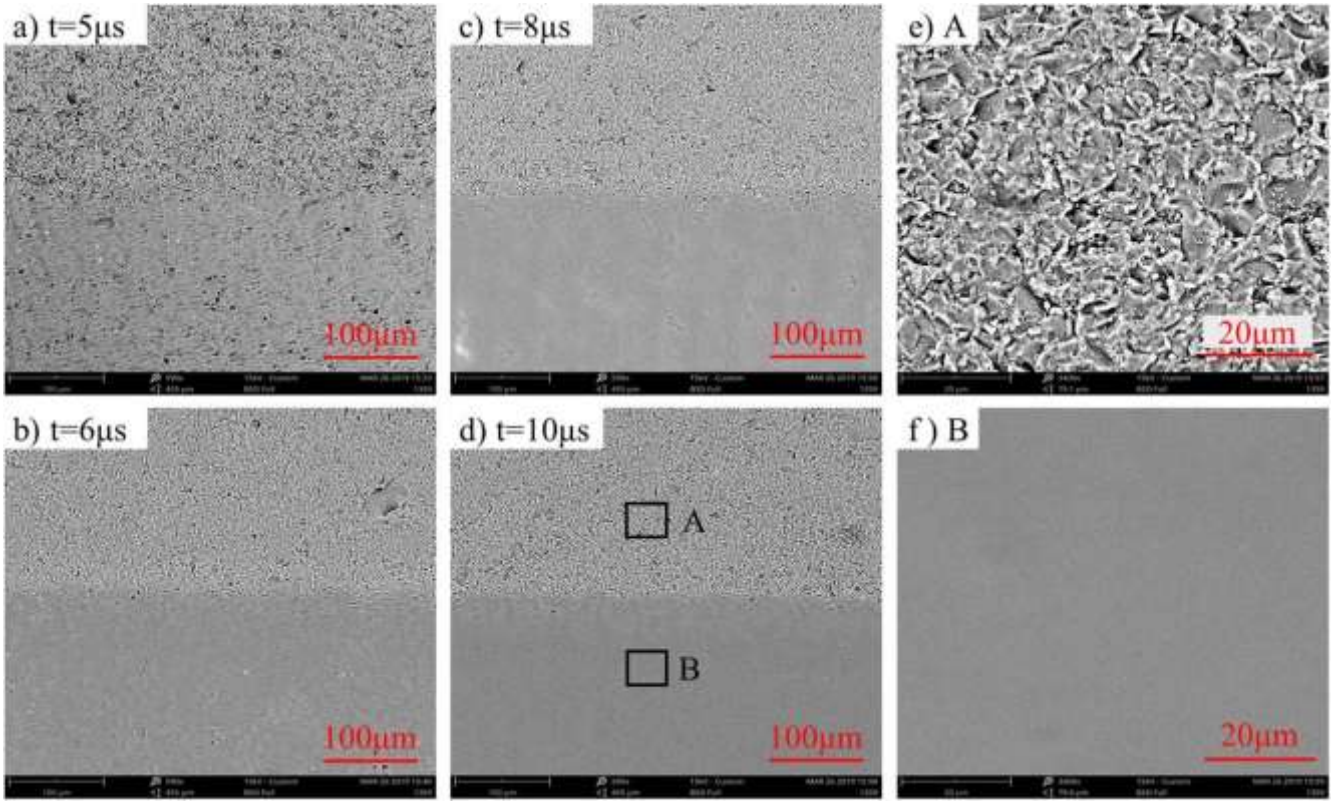

Figure 11. Surface measurements by SEM: laser polishing surface with pulse width of (a) 5 μs, (b) 6 μs, (c) 8 μs, and (d) 10 μs; (e) initial fine-ground surface; (f) detailed view of laser polishing surface with a pulse width of 10 μs.

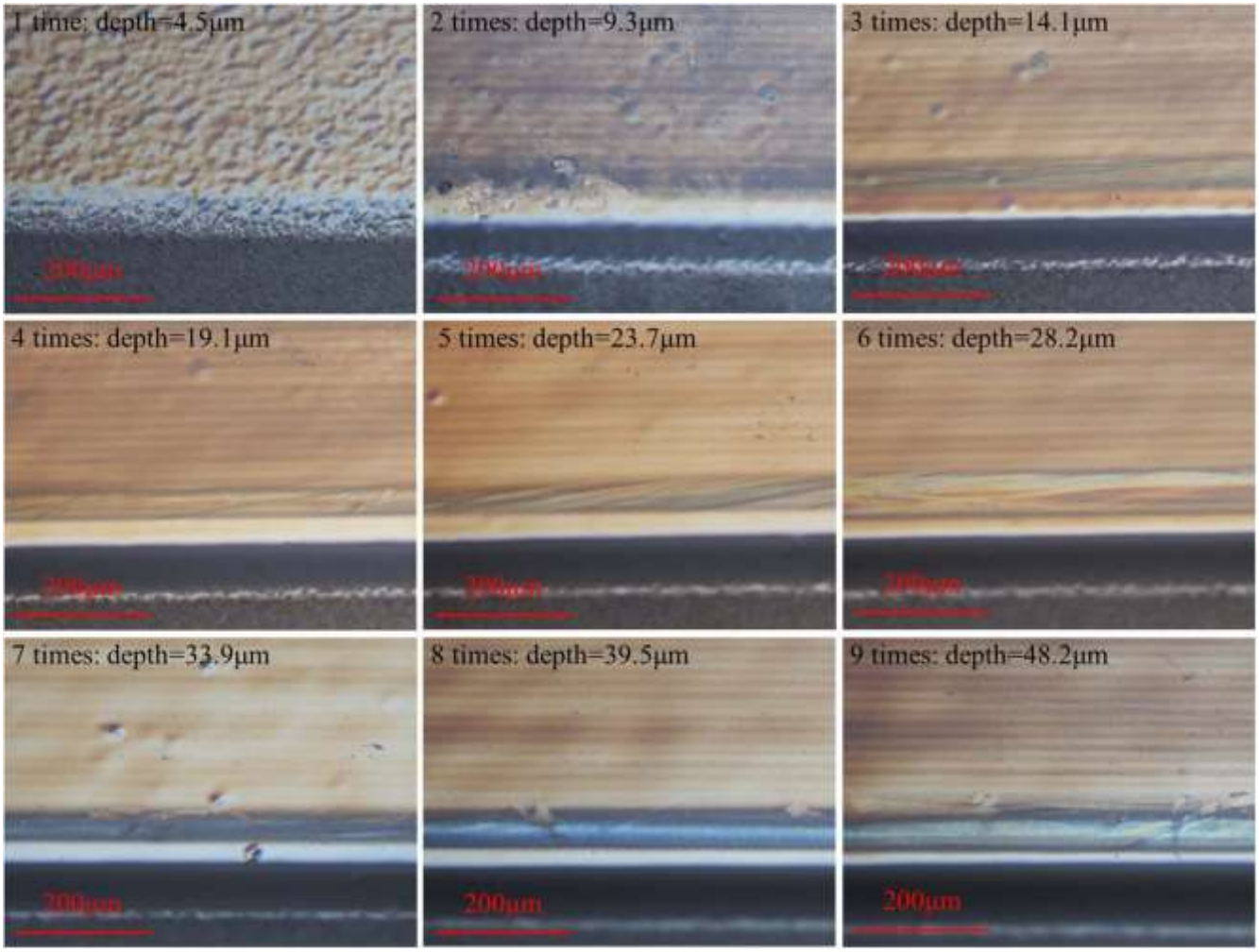

Figure 12. Surface measurements by high-magnification optical microscope: surface with polishing times from one to nine and pulsed

figures 11(a) and (b). When the pulse width was greater than 8 μs, the surface became very smooth and cracks disappeared, as shown in figures 11(c)–(f).

The removal depth of the material was several microns, which verified that surface defects can be removed by CO_2 laser polishing and a smooth surface in local area was formed. Therefore, it was necessary to further verify the ability of CO_2 laser polishing to remove subsurface defects. The fused silica optics with a surface roughness of 250 nm after grinding were divided into several zones. The number of polishing times of each zone was different. The polishing depth was measured by a profile-meter. The surface quality was observed by high-magnification optical microscope.

Figure 12 showed the surface measurements by high-magnification optical microscope after laser polishing with the number of polishing times from 1 to 9. The experimental parameters of the laser with power at 50 W, frequency of 10 kHz, pulse width of 10 μs, pulsed distance of 20.7 μm, and track pitch of 17.3 μm were used to polish fused silica. In the first laser polishing, the polishing depth is 4.5 μm and the surface roughness is reduced to 100 nm. However, there are many pits on the polished surface. With the increase of polishing times, the polishing depth increased and the number of

pits on the polished surface decreased rapidly. When the polishing times reached six, the polishing depth was 28.2 μm, and there were no pits on polished surface. However, several pits were observed when the number of polishing times reached seven.

In fact, the depth of CO_2 laser polishing must be greater than the actual defect depth in order to guarantee that the sub- surface defect can be removed. According to reported results
[27], the subsurface defects of the ground fused silica optics were distributed in the depth of 1–100 μm. However, the depth of the subsurface was related to the grinding process. When thepolishing depth of the sample used in this experiment was
greater than 40 μm, no pits can be observed on the processed surface. This means that the subsurface defects in the processed area had been completely removed. Therefore, the depth of the subsurface defects in the processed area was less than 40 μm. Byoptimizing the parameters, the deeper polishing depth and bettersurface quality can be achieved.

Table 3 showed polishing rates with different processing parameters and scanning polishing was performed with a smallbeam CO_2 laser in a given processing area (2 × 2 mm^2). The result showed that the polishing depth of the material increased with the increase of polishing times. However, the change of

Table 3. Polishing rate of CO_2 laser polishing fused silica optics.

Times	Area (mm^2)	Depth (μm)	Time (s)	Polishing rate ($\mu m\ s^{-1}$)
1	2 ×2	4.5	1.382	3.26
2	2 ×2	9.3	2.764	3.36
3	2 ×2	14.1	4.146	3.40
4	2 ×2	19.1	5.528	3.46
5	2 ×2	23.7	6.91	3.43
6	2 ×2	28.2	8.292	3.40
7	2 ×2	33.9	9.674	3.50
8	2 ×2	39.5	11.056	3.57
9	2 ×2	48.2	12.438	3.88

material removal depth per second was very small, which was defined as polishing rate. Obviously, it was an average polishing rate. The maximum material polishing rate was 3.88 $\mu m\ s^{-1}$, which was much higher than that of traditional mechanical polishing. In the CO_2 laser polishing, the polishing depth can be quantified and subsurface defects can be removed completely.

Therefore, the surface and subsurface defect were removed quickly and a defect-free surface was formed by rapid CO_2 laser polishing. CO_2 laser polishing can be applied as an alternative process for precision polishing of fused silica. By combining rapid laser polishing with ultra-precision processing (such as magnetorheological polishing, ion beam polishing), the ultra-smooth, defect-free surface will be processed, which can greatly improve the ultra-precision polishing efficiency of fused silica optics.

5. Conclusions

As an advanced manufacturing technique, CO_2 laser polishing is widely used in processing fused silica optics. In this study, the formation of a smooth, defect-free surface of fused silica was investigated using rapid CO_2 laser polishing. A numerical model for describing the CO_2 laser polishing of fused silica with coupled multiple beams was established. The forming mechanism of a smooth defect-free surface on fused silica optics by laser polishing was theoretically established. The effects of laser polishing parameters, such as overlap rate, pulse width and polishing times, on the polishing quality were experimentally investigated. The theoretically calculated polishing depth was in close agreement with the experimental results. The experimentally measured period and height of residual micro-ripples on polished surface were in agreement with the simulation results as well. When the material removal depth reached 2414 nm, the roughness *Ra* of the processed surface was better than 25 nm. Besides, the surface cracks introduced by prior grinding process were removed by laser polishing and a defect-free surface was achieved. The maximum material polishing rate reached 3.88 $\mu m\ s^{-1}$, much higher than that of traditional mechanical polishing methods. Therefore, the rapid CO_2 laser polishing technique can be applied as an alternative process for precision polishing of fused silica optics. It can effectively achieve smooth, defect-

free surface, which is of great significance in improving the surface quality of fused silica optics applied in high-power laser facilities. However, with thermal processing mechanism, residual stress and surface distortion are the two major challenges of CO_2 laser polishing. Therefore, it is necessary to optimize the processing parameters to achieve smaller surface distortion, and meanwhile carry out thermal annealing post- processing process to remove residual stress in the future work. This will further promote the application of rapid CO_2 laser polishing technique in high-power laser facilities.

References

[1] Kaiser N, Stolz C J, Lequime M and Macleod H A 2008 Statusof NIF mirror technologies for completion of the NIF facility*Proc. SPIE* 7101 710115
[2] Moses E I 2008 The national ignition facility (NIF): a path to fusion energy *Energy Convers. Manage.* 49 1795
[3] Campbell J H *et al* 2004 NIF optical materials and fabrication technologies: an overview *Proc. SPIE* 5341 84
[4] Norton M A *et al* 2007 Growth of laser damage in fused silica:diameter to depth ratio *Proc. SPIE* 6720 67200H
[5] Menapace J, Bude J D, Wong L L, Feit M D, Shen N, Miller P E, Laurence T A, Suratwala T I and Steele W A
2010 Fracture-induced subbandgap absorption as a precursor to optical damage on fused silica surfaces *Opt. Lett.* 35 2702–4
[6] Laurence T A, Bude J D, Shen N, Feldman T, Miller P E, Steele W A and Suratwala T 2009 Metallic-like photoluminescence and absorption in fused silica surface flaws *Appl. Phys. Lett.* 94 1039
[7] Bass I L, Guss G M, Nostrand M J and Wegner P J 2010 Animproved method of mitigating laser-induced surface damage growth in fused silica using a rastered pulsed CO_2laser *Proc. SPIE* 7842 784220
[8] Folta J *et al* 2013 Mitigation of laser damage on national ignition facility optics in volume production *Proc. SPIE*8885 88850Z
[9] Li Y, Ye H, Yuan Z, Liu Z, Zheng Y, Zhang Z, Zhao S, Wang J and Xu Q 2016 Generation of scratches and their effects on laser damage performance of silica glass *Sci. Rep.*6 34818

[10] Cormont P, Bourgeade A, Cavaro S, Doualle T, Gaborit G, Gallais L, Rullier J-L and Taroux D 2015 Process for repairing large scratches on fused silica optics *Proc. SPIE* 9633 96330A
[11] Robin L, Combis P, Cormont P, Gallais L, Hebert D, Mainfray C and Rullier J-L 2012 Infrared thermometry and interferential microscopy for analysis of crater formation at *J. Appl. Phys.* 111 063106
[12] Jung S, Lee P A and Kim B H 2016 Surface polishing of quartz-based microfluidic channels using CO_2 laser *Microfluid. Nanofluid.* 20 84
[13] Serhatlioglu M, Ortaç B, Elbuken C, Biyikli N and Solmaz M E 2016 CO_2 laser polishing of microfluidic channels fabricated by femtosecond laser assisted carving *J. Micromech. Microeng.* 26 115011
[14] Wlodarczyk K L, Weston N J, Ardron M and Hand D P 2016 Direct CO_2 laser-based generation of holographic structures on the surface of glass *Opt. Express* 24 1447
[15] Zhang C C, Liao W, Zhang L J, Jiang X L, Chen J, Wang H J, Luan X Y and Yuan X D 2018 Large-area uniform periodic microstructures on fused silica induced by surface phonon polaritons and incident laser *Opt. Lasers Eng.* 105 101
[16] Heidrich S, Richmann A, Schmitz P, Willenborg E, Wissenbach K, Loosen P and Poprawe R 2014 Optics manufacturing by laser radiation *Opt. Lasers Eng.* 59 34
[17] Weingarten C, Uluz E, Schmickler A, Braun K, Willenborg E, Temmler A and Heidrich S 2017 Glass processing with pulsed CO_2 laser radiation *Appl. Opt.* 56 777
[18] Weingarten C, Schmickler A, Willenborg E, Wissenbach K and Poprawe R 2017 Laser polishing and laser shape correction of optical glass *J. Laser Phys.* 29 011702
[19] Doualle T, Gallais L, Cormont P, Donval T, Lamaignère L and Rullier J L 2016 Effect of annealing on the laser induced damage of polished and CO_2 laser-processed fused silica surfaces *J. Appl. Phys.* 119 213106
[20] Laurent G, Philippe C and Jean-Luc R 2009 Investigation of stress induced by CO_2 laser processing of fused silica optics for laser damage growth mitigation *Opt. Express* 17 23488
[21] Doualle T, Gallais L, Cormont P, Hébert D, Combis P and Rullier J L 2016 Thermo-mechanical simulations of CO_2 laser–fused silica interactions *J. Appl. Phys.* 119 113106
[22] Nowak K M, Baker H J and Hall D R 2015 Analytical model for CO_2 laser ablation of fused quartz *Appl. Opt.* 54 8653
[23] Elhadj S, Matthews M, Yang S and Cooke D J 2012 Evaporation kinetics of laser heated silica in reactive and inert gases based on near-equilibrium dynamics *Opt. Express* 20 1575
[24] Markillie G A J, Baker H J, Villarreal F J and Hall D R 2002 Effect of vaporization and melt ejection on laser machining of silica glass micro-optical component *Appl. Opt.* 41 5660
[25] Zhao J, Sullivan J, Zayac J and Bennett T D 2004 Structural modification of silica glass by laser scanning *J. Appl. Phys.* 95 5475
[26] Mendez E, Nowak K M, Baker H J, Villarreal F J and Hall D R 2006 Localized CO_2 laser damage repair of fused silica optics *Appl. Opt.* 45 5358
[27] Spaeth M L *et al* 2016 Optics recycle loop strategy for NIF operations above UV laser-induced damage threshold *Fusion Sci. Technol.* 69 265